# Preparation of High-Purity Amorphous Silica from Colored Glass Waste using the Alkaline Fusion Method

**Fadia W. Al-Halfi *& Harith A. Al-Saad**

Department of Geology, College of Science, University of Basrah, Basrah, Iraq.

***Corresponding author E-mail:** fadia.waleed@uobasrah.edu.iq

**https://doi.org/10.29072/basjs.20260215**

**ARTICLE INFO**

*Received: 21 May 2026*

*Accepted: 13 July 2026*

*Published: 31 August 2026*

This article is an open access article distributed under the terms and conditions of the Creative Commons Attribution-NonCommercial 4.0 International (CC BY-NC 4.0 license) http://creativecommons.org/licenses/by-nc/4.0//).

***Keywords:***

*Colored glass waste, Recycling Alkali fusion, High-purity silica, Surface area*

**ABSTRACT**

High-purity silica is valuable in modern industries. Colored glass waste, however, is an environmental pollutant and difficult to recycle. Therefore, silica from sustainable sources presents both industrial and environmental challenges. The study aims to convert this waste into silica using the alkaline fusion method (an economical, relatively low-temperature method). The methodology involved immersing crushed waste glass in 2M HCl for 24 hours. Solid sodium silicate was formed by heating 20 g of purified waste glass with 80 g of NaOH at 500 C° for 2 hours. Sodium silicate solution and 3M HCl were mixed to prepare silicic acid. The aging took 18 hours, followed by filtering and 48 hours of drying. XRD confirmed the product's amorphous nature. Chemical analysis revealed that the final product contained 99% silica, compared to 69.94% in raw glass waste, with a yield rate of 98.59%. There was a significant decrease in impurities ($Fe_2O_3$, $Al_2O_3$, MgO, and $SO_3$). BET analysis showed a specific surface area (53.04 $m^2/g$) and a low total pore volume (0.263 $cm^3/g$). BJH analysis confirmed the mesoporous nature, with pore volumes of 0.261 $cm^3/g$ and mesopore surfaces of 52.93 $m^2/g$. This process was stable across all waste glass colors, indicating potential for industrial and nanoporous material applications.

## 1. Introduction

Soil pollution is one of the most serious environmental challenges facing the modern world. Land degradation is characterized by the loss of environmental and economic value due to excessive human activity or pollution **[1]**. Among the factors contributing to this problem are waste management practices, particularly the irresponsible disposal of non-biodegradable materials such as glass, plastics, and aluminum cans. Glass waste takes thousands of years to decompose naturally in landfills, which depletes large areas of land and contaminates soil and groundwater with heavy metals such as cobalt, chromium, and iron **[2-3]**.

Globally, glass production exceeds 130 million tons each year, contributing approximately 30–35 million tons of post-consumer waste; 60–70% of this waste ends up in landfills **[4]**. In this waste stream, mainly colored glass— green, brown, and white— constitutes the majority, although mixed colors often prove difficult to recycle using conventional methods **[5-6]**. In Iraq, glass waste management is underdeveloped, and there is no large-scale recycling infrastructure. The beverage, food, and construction industries in Basra generate significant volumes of glass waste, but it is either landfilled or disposed of informally. There is a pressing need to develop locally applicable valorization pathways for glass waste **[7]**. As global production of these materials continues to increase, their disposal in landfills has become unsustainable from an environmental and economic standpoint. As a result, recycling is one of the most effective methods for reducing the environmental impact of this waste and converting it into a valuable economic resource **[8]**. Recycling glass not only conserves energy—using 20% to 30% less energy than producing new glass from raw materials—but also preserves natural resources by reducing the need to extract sand, limestone, and sodium carbonate **[9]**. Additionally, it lowers greenhouse gas emissions by decreasing the carbon dioxide released during melting **[10-11]**. Nonetheless, the presence of metal oxides like iron, cobalt, chromium, and copper can pose significant challenges to the glass recycling process. For instance, mixing colored glass with transparent glass significantly reduces the final product's quality **[12]**. After examining the colored glass problem, it is critical to note that colored beverage bottles, light bulbs, and laboratory glassware are rich in silica and can serve as alternative silica sources **[13]**. The use of high-purity silicon dioxide extends beyond traditional containers for beverages, window glass, and household items to advanced industrial and biotechnology fields like fiber optics (the backbone of communication and internet networks), optical glass (used in lenses and telescopes), and pharmaceuticals and cosmetics (as a filler and property enhancer) **[14-15]**. As a result of these expansions in applications, the demand for ultra-pure silica is increasing, which

has led to a growing interest in finding sustainable and alternative sources of silica for production, rather than relying on limited natural sands that require costly and environmentally damaging mining operations **[16]**.

In terms of preparation methods, researchers have developed several approaches for producing high-purity silica, which differ in their chemical principles, costs, efficiency, and suitability to different raw materials **[17-19]**. Among these methods are sol-gel processing, electrocoagulation **[20]**, hydrothermal treatment **[21]**, and alkaline fusion **[22]**. Sol-gel processing produces high-purity silica with precise control of pore structure, it is expensive and requires toxic organic raw materials such as tetraethoxysilane **[23]**. High-purity silica can also be obtained by hydrothermal treatment, but it requires specialized equipment that operates at high pressures and temperatures, resulting in high energy consumption and costs **[24]**. However, electrocoagulation has low productivity, and it is only suitable for aqueous solutions, not solids **[16]**. Raw material availability and ease of application are key features of the alkaline fusion method. Low-cost alkaline reagents such as NaOH, KOH, or $Na_2CO_3$ are used to moderate the temperature in sand at a relatively moderate temperature (500 $C^{\circ}$) to produce soluble sodium silicate, which is subsequently converted into silica, which is suitable for processing silica-rich materials like recycled glass and sand **[25]**.

Several previous studies emphasized extracting silica from rice husks **[26-27]**, fly ash **[28]**, and clear glass **[29]**. However, colored glass waste has attracted relatively little attention because metal oxide colorants make silica recovery more challenging. **[16]** reported that high-purity $SiO_2$ (99.9%) could be extracted from colored glass using NaOH fusion. In contrast, the study adopted a high NaOH ratio (90%) and did not address extensive structural characterization, process optimization, or potential applications.

The present study aims to overcome these limitations. First, introducing an acid pre-treatment step improves raw material quality and reduces NaOH utilization, thereby lowering chemical use, production costs, and environmental impacts. Second, the extracted silica is characterized using X-ray Diffraction, X-ray Fluorescence, Brunauer-Emmett-Teller, and Barrett-Joyner-Halenda. Third, the study focuses on developing functional silica materials with potential value-added applications rather than conventional recycling. Accordingly, by using colored glass as a waste resource, this study aims to fill a research gap by producing high-purity amorphous silica with an enhanced, simplified, and cost- effective version of the alkali fusion method.

## 2. Materials and Methods

### 2.1. Raw Materials

Waste glass of diverse colors, including green, white, and brown, was collected from the Rafaaiya sanitary landfill, located approximately 45 to 50 kilometers from the Basrah Governorate in southern Iraq (**Figure 1**). Also used were hydrochloric acid (HCl) at 37%, sodium hydroxide (NaOH) in granular form (99% purity), and distilled water.

The equipment included a 250 mL glass beaker, a graduated cylinder, a pipette, a funnel, an RM 200 grinder, a pH meter, a thermometer, a Whatman No. 41 filter paper, a drying oven, a precision analytical balance, and a muffle furnace for heating.



**Figure 1.** Colored glass waste collected from Basrah Governorate, Southern Iraq.

The methodology consisted of several sequential stages, as described below.

### 2.2. Acid Pre-treatment

Initially, glass waste was washed with distilled water to remove soil and other contaminants. Then, it was exposed to sunlight for 24 hours until completely dry. Subsequently, the dried glass was ground using an RM 200 grinder and passed through a 63 μm sieve **[30]** to reduce the particle size and increase the surface area between the solute and the solvent **[31]**. The grinding process was conducted at the Department of Geology, College of Science, University of Basrah, Iraq (**Figure 2**).

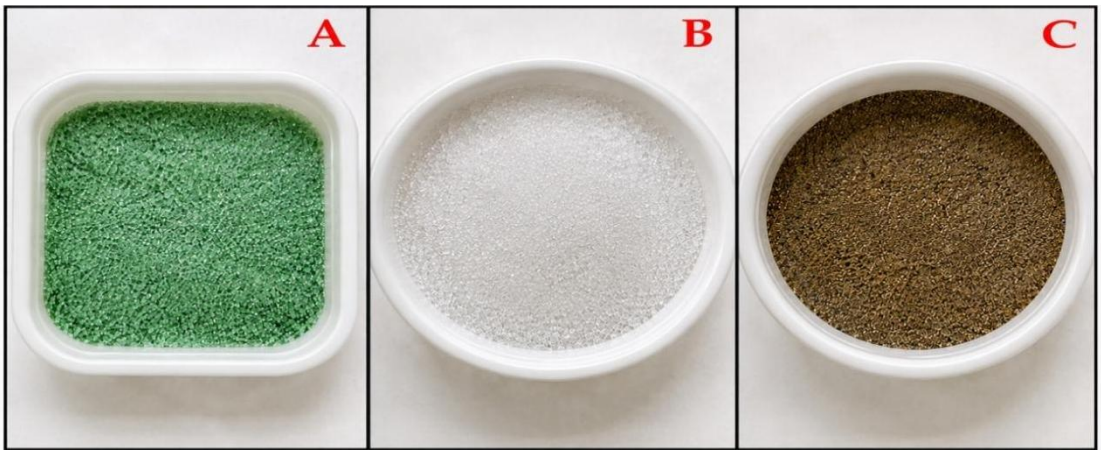



**Figure 2.** Different colors of crushed glass waste (A: green, B: white, and C: brown).

### 2.2. Characterization of Colored Glass Waste

X-ray diffraction (XRD) was used to identify the crystalline phases in the green, white, and brown waste glass powders (Department of Physics, College of Science, University of Basrah, Iraq). Analysis was conducted with Cu Kα radiation (λ = 1.5406 Å), operating at 40 kV and 30 mA, with a scanning range of 10–80° (2θ). The samples were analyzed using an ED-XRF Spectro XEPOS system developed by Australian Laboratory Services (ALS). In accordance with the factory calibration protocol, the X-ray tube was operated under standard excitation conditions and vacuum.

### 2.4. Alkaline Fusion Method

A 25 g sample of waste glass powder was immersed in 30 mL of 2 M HCl for 24 h, stirring manually every 30 min to enhance the solute-solvent interaction and maintain a proper solid-to-liquid ratio. As reported in **[32]**, 2 M HCl can reduce CaO by 13% and increase $SiO_2$ by 17%. **[29, 33]** recommend a 24 hours immersion because of diffusion limitations. Mass transfer is enhanced when the mixture is stirred every 30 min, as documented in **[34]**. Whatman No. 41 Filter paper was used to filter the soaked samples, and distilled water was used to rinse them until the pH reached 7–8. They were then dried at 100 C° for 2 h **[35]**. After recovering the purified glass powder, 20 g of this purified glass powder were taken for further processing. Next, solid sodium silicate was prepared by heating a mixture of 20 g of purified glass powder and 80 g of NaOH (99% purity). The mixture was heated to 500 C° in a programmable furnace at 2.5 C°/min at room temperature. It was held at this temperature for 2 hours **[36] (Figure 3)**. A 1:4 ratio of glass to NaOH was used to dissolve the amorphous silicate network completely.

According to **[37]**, sodium silicate solutions can be produced in an adjustable ratio. The ratio provides the foundation for converting glass into soluble sodium silicate in a quantitative manner. By adding distilled water to solid sodium silicate, a sodium silicate solution was obtained (**Figure 4**).

To prepare the silicic acid, the sodium silicate solution was gradually mixed with 3 M HCl until a white gel-like substance (at pH 1–2) was obtained. The remaining dissolved salts were removed by washing silicic acid using 300 mL of distilled water, ten times, as described in **[22]**. After 18 hours of aging, the gel mixture was filtered through filter paper and dried in a hot-air oven at 110 C° for 48 hours **[38]**. As a last step before analyses, the manufactured silica agglomerates were milled using an RM 200 grinder (**Figure 5**).




**Figure 3.** Solid sodium silicate prepared from purified colored glass waste (A: green, B: white, and C: brown).



**Figure 4.** Sodium silicate solution from purified colored glass waste (A: white, B: green, and C: brown)




**Figure 5.** White silica made by processing colored glass waste via the alkaline fusion method

### 2.5. Characterization of Produced Silica

Utilizing XRD and XRF techniques, the silica product was identified and evaluated. The specific surface area of the prepared silica was also determined at the University of Tehran, Iran, using a BET Prep VAC II instrument. The instrument operates on nitrogen ($N_2$) adsorption–desorption measurements. Before analysis, the samples were degassed under vacuum heating conditions to remove moisture and adsorbed impurities. The BET analysis was conducted under standard operating conditions using nitrogen as the adsorbate gas **[32]**. The BJH analysis is applied to the desorption branch of the nitrogen adsorption isotherm to determine pore size distributions and mesopore characteristics. A BJH analysis was performed on synthesized silica to determine its pore volume and pore surface area **[39]**. Silica nanoparticle yield rates can be calculated using the following Equation (10), according to **[40]**.

$$\text{Yield (\%)} = \frac{\text{weight of the extracted silica powder (g)} \times \text{P synthetic silica}}{\text{weight of the raw waste glass (g)} \times \text{Pglass}} \text{ ------ (1)}$$

$P_{glass}$ = fraction of $SiO_2$ in raw waste glass (determined by XRF analysis)

$P_{synthetic\ silica}$= fraction of $SiO_2$ in synthetic purity silica (determined by XRF analysis)

## 3. Results and Discussion

### 3.1. Raw Colored Glass Waste

#### 3.1.1. Mineral Analysis of Raw Colored Glass Waste

XRD analysis was performed over a 2-theta range of 2–60°. No sharp Bragg peaks were observed in any of the raw glass waste samples (white, green, or brown), indicating their amorphous nature and similar structural characteristics **[41-45] (Figure 6**).

Nevertheless, low-intensity reflections are observed between 31 and 33°, which may be due to baseline effects or residual trace crystallizations and do not affect the overall amorphous nature of the samples.

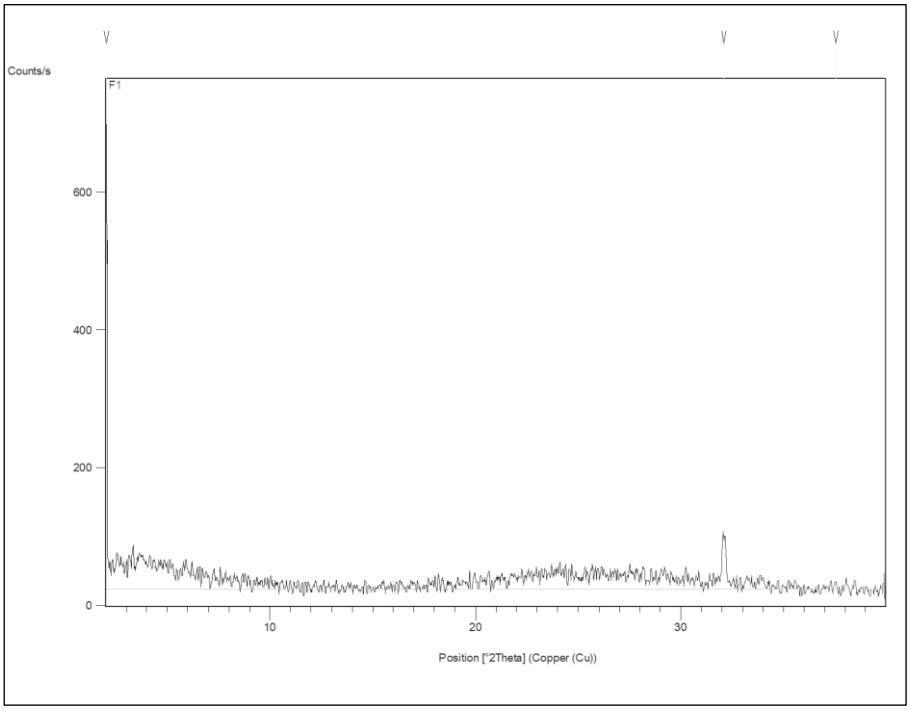



**Figure 6.** Mineral analysis of raw colored glass waste

### 3.1.2. Chemical Analysis of Raw Colored Glass Waste

The chemical compositions of colored glass waste show that the highest silica ($SiO_2$) content was in white glass (71.11%), followed by green glass (69.75%), and the lowest was in brown glass (68.95%). Brown glass had the highest $Al_2O_3$ + $Fe_2O_3$ content (4.90%) and MgO content (7.01%). A slight increase in $SO_3$ levels were also detected in green and brown glass (0.17% and 0.19%, respectively) compared to white glass (0.15%), as shown in Table 1 and (Figure 7**)**.

These variations in chemical composition can be explained by the contribution of transition metal oxides throughout production. Transition metal oxides are added during the manufacturing process to absorb specific wavelengths of light and create the desired color **[46]**. These oxides are present in low proportions in white glass, which maintains transparency. Iron ($Fe_2O_3$) contributes to the green color in large quantities, while chromium may also contribute, although it is not quantified in the present study **[47]**. Iron and sulfur ($SO_3$) react in brown glass, forming iron sulfide (FeS), which gives its brown color **[48]**. To enhance mechanical qualities or enable the incorporation of coloring additives without crystallizing, many modified oxides are used **[49]**.

**Table 1.** The chemical composition of colored glass waste samples

| Chemical Composition | Glass Waste % | | | Average % |
|---|---|---|---|---|
| | White | Green | Brown | |
| **$SiO_2$** | 71.11 | 69.75 | 68.95 | **69.94** |
| **$Al_2O_3 + Fe_2O_3$** | 4.3 | 4.5 | 4.9 | **4.57** |
| **CaO** | 7.55 | 7.6 | 7.49 | **7.55** |
| **$SO_3$** | 0.15 | 0.17 | 0.19 | **0.17** |
| **$Na_2O + K_2O$** | 10.5 | 10.87 | 10.69 | **10.69** |
| **MgO** | 6.09 | 6.98 | 7.01 | **6.69** |

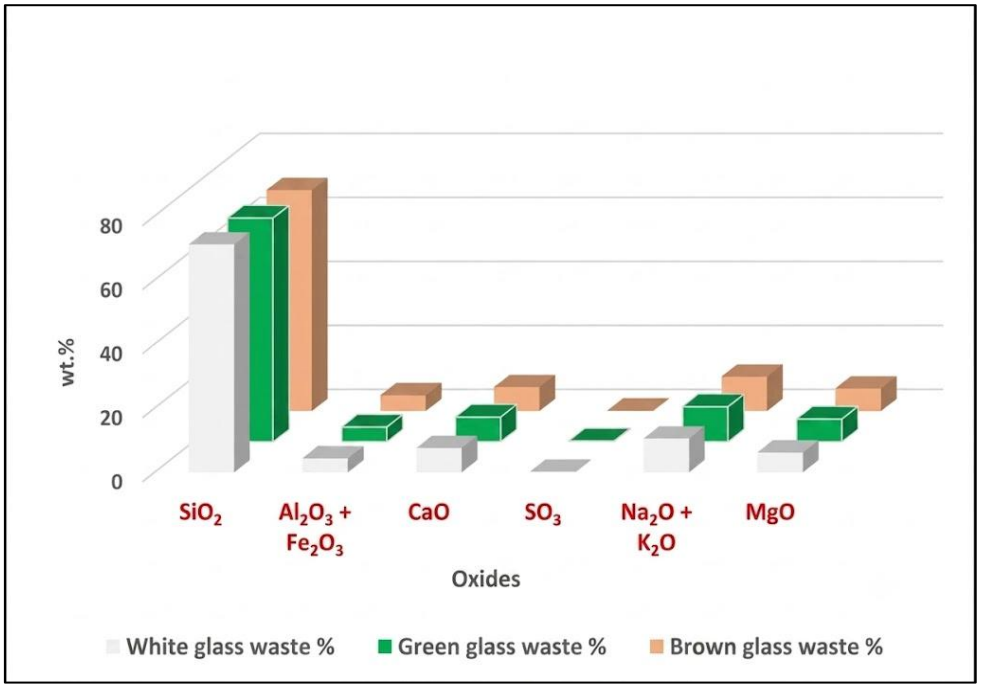



**Figure 7.** A comparison of oxides weight percentages in raw colored glass waste

### 3.2. Reaction Mechanism

The alkaline fusion method for recycling colored glass waste into high-purity silica involves three sequential chemical reactions.

First, the alkaline fusion method breaks down the glass network, which is composed of interconnected siloxane (Si-O-Si) bonds. Hydroxide ions dismantles the three-dimensional silica framework, transforming it into soluble sodium silicate materials, as shown in Equation (2). This change increases silica's solubility and facilitates extraction **[50]**.

**$2NaOH + SiO_2 \rightarrow Na_2SiO_3 + H_2O$ ---------- (2)**

Second, when hydrochloric acid is added to soluble silicate materials, silicic acid [$Si(OH)_4$] is formed, and sodium chloride is produced as a byproduct Equation (3) **[50]**

**$Na_2SiO_3 + H_2O + 2HCl \rightarrow Si(OH)_4 + 2NaCl$ ---------- (3)**

The third reaction is condensation, which occurs when deprotonated silanol groups (Si-O) attack neutral $Si(OH)_4$ molecules. It creates new siloxane bonds (Si–O–Si) and initiates the formation of a three-dimensional hydrated silica network. Gel structure is determined by pH, temperature, and aging time, which regulate condensation rate and pore architecture. When dried, amorphous silica with a specific surface area and a mesoporous structure is obtained **[51]**. Finally, the reaction shows that silicic acid loses water thermally at 110 C°, forming amorphous silica ($SiO_2$) and water vapor. Equation (4) illustrates this.

**$Si(OH)_4 \rightarrow SiO_2 + 2H_2O$ ---------- (4)**

### 3.3. Characterization of High-Purity Silica

#### 3.3.1. Mineral Analysis of High-Purity Silica

X-ray diffraction analysis of the silica produced by the alkali fusion process revealed a broad peak centered at approximately 22° (2θ) and a flat baseline; no significant crystalline reflections were detected (**Figure 8**), which confirms that the resulting silica is amorphous **[52].**

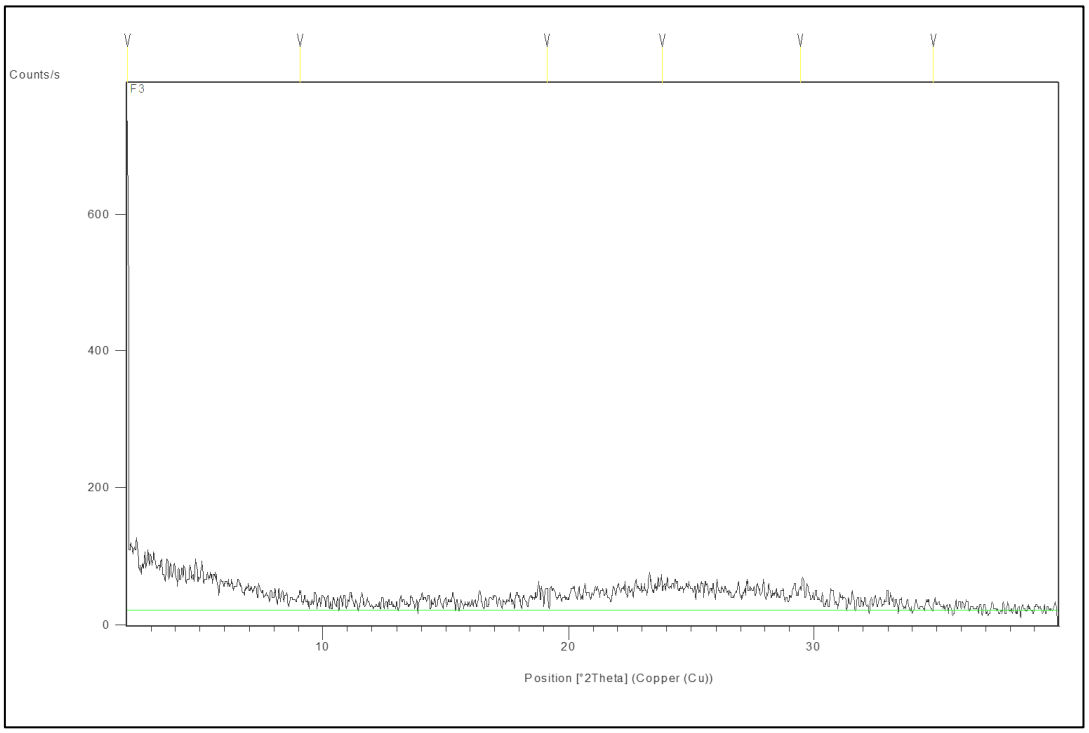



**Figure 8**. X-ray diffraction pattern of the silica product

### 3.3.2. Chemical Analysis of High-Purity Silica

Chemical analysis of the produced silica showed that alkaline fusion effectively purifies silica and removes impurities from colored glass waste, regardless of the original glass color (white, green, or brown). $SiO_2$ average increased from 69.94% in raw glass waste to 99% in the final product. In contrast, associated impurities ($Fe_2O_3$, $Al_2O_3$, MgO, $SO_3$) decreased to less than 1% (**Figure 9**) (**Table 2**).

The presence of approximately 1% $Fe_2O_3$ in the final product can be explained by the incomplete removal of iron-containing impurities during the purification process. These residual iron oxides may originate from insoluble phases that are difficult to eliminate under the applied chemical treatment conditions. Compared with **[32]**, which investigated silica extraction from dune sands, the alkaline smelting method produced high-purity silica (86.3%), although trace amounts of iron impurities were detected. It appears that, despite using different raw materials, the complete removal of iron oxide remains a challenge**.** The XRF analysis results demonstrated that the silica purity was about 99% $SiO_2$ with a very low content of alkali metal oxides ($Na_2O + K_2O \leq 0.007$ wt.%), indicating the effectiveness of the washing process and the removal of sodium chloride residue, even though no electrical conductivity measurements were carried out.

**Table 2.** Chemical analysis of synthetic silica

| Chemical composition | Produced silica from waste glass | | | Average % |
|---|---|---|---|---|
| | White | Green | Brown | |
| $SiO_2$ | 99.01 | 98.95 | 98.94 | 99.00 |
| $Al_2O_3 + Fe_2O_3$ | 0.98 | 1.001 | 1.004 | 0.995 |
| CaO | 0.001 | 0.002 | 0 | 0.000667 |
| $SO_3$ | 0 | 0 | 0 | 0 |
| $Na_2O + K_2O$ | 0.001 | 0.01 | 0.003 | 0.007 |
| MgO | 0.003 | 0.005 | 0 | 0.000667 |

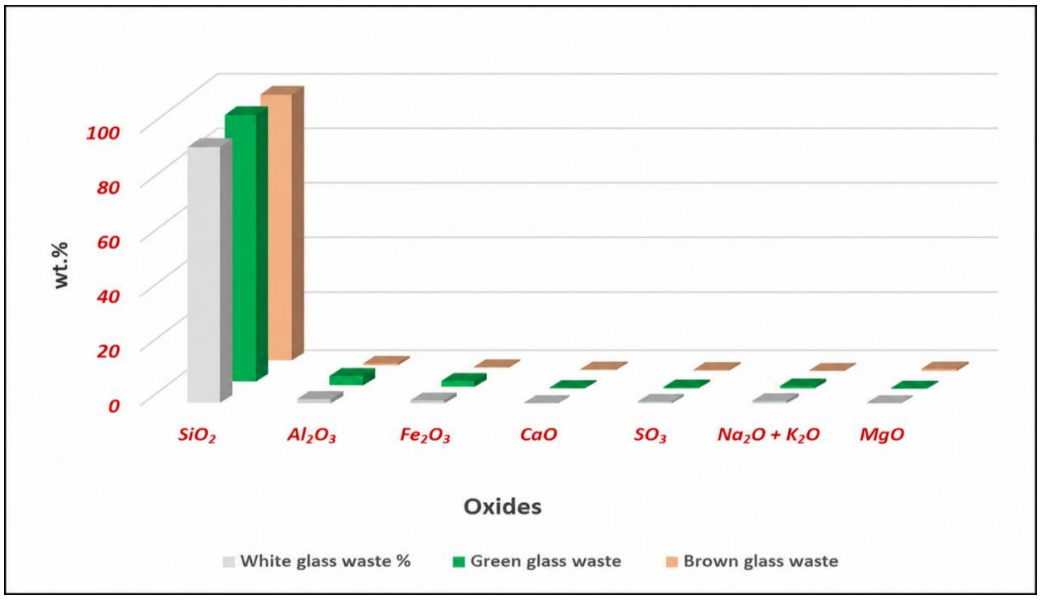



**Figure 9.** A comparison of oxide weight percentages in synthetic silica

### 3.4. Specific Surface Area of Synthetic Silica

BET analysis revealed that the synthetic silica has a specific surface area of 53.04 $m^2/g$, a monolayer volume of 68.5 $cm^3/g$, and a total pore volume of 0.263 $cm^3/g$ as determined by nitrogen gas adsorption (**Table 3)**. The average particle size of 9.02 nm falls into the nanosized range that precipitated amorphous silica, which is consistent with what was reported by **[53-54]**.

BJH method yielded a mesopore surface area of 52.93 $m^2/g$, and a pore volume of 0.261 $cm^3/g$.

The study found that silica produced from different colored glass waste has almost identical surface areas and pore volumes, which indicates that the process is consistent regardless of the glass color.

**Table 3** An analysis of the surface characteristics of amorphous silica with BET and BJH :

| BET | | | BJH | | |
|---|---|---|---|---|---|
| **Total pore volume ($cm^3/g$)** | **Monolayer volume ($cm^3/g$)** | **Average particle size (nm)** | **Specific surface area ($m^2/g$)** | **Pore Volume ($cm^3/g$)** | **Mesopore Surface Area ($m^2/g$)** |
| 0.263 | 68.5 | 9.02 | 53.04 | 0.261 | 52.93 |

BJH analysis was employed to assess the porous structure of the obtained high-purity silica. **Figure 10** displays that the pore size distribution (dV/dr–p) vs (r–p) exhibits a distinct peak at

a pore radius of 1.21 nm, equating to a pore diameter of roughly 2.42 nm. This measurement aligns with the IUPAC classification for average pore sizes (2–50 nm), verifying the mesoporous characteristic of the extracted silica. According to BJH analysis, the average pore surface area was 52.93 $m^2/g$, and the corresponding pore volume was 0.261 $cm^3/g$. A narrow distribution of pore sizes is a characteristic of mesoporous structures. The BET measurement, which revealed a mean particle size of 9.02 nm and a specific surface area of 53.04 $m^2/g$, further suggests that the material possesses nanoscale characteristics in light of these findings.

**Figure 11** illustrates the nitrogen adsorption–desorption curve for high-purity silica. According to the IUPAC classification, this curve displays a Type IV pattern, typical of mesoporous substances. The adsorption and desorption branches align closely throughout the full range of relative pressure ($P/P_0$ = 0.0–1.0), indicating either open cylindrical pores or a structure dominated by the surface.

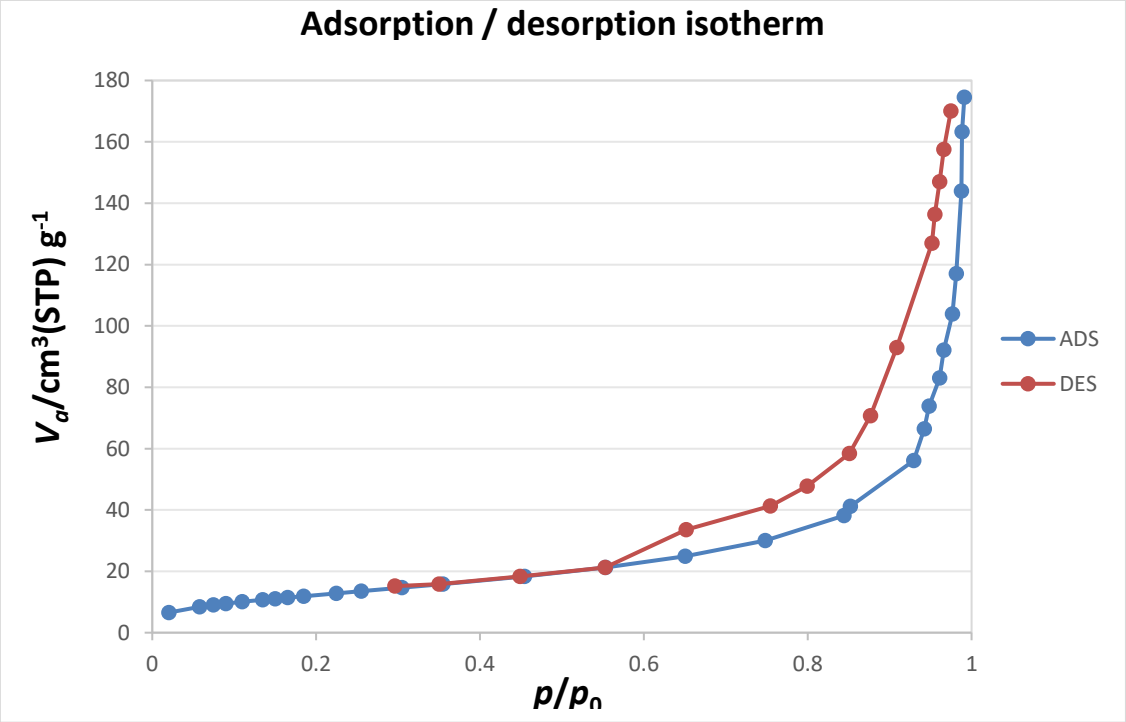



**Figure 10.** A desorption isotherm showing the pore size distribution of synthetic silica created from waste glass.

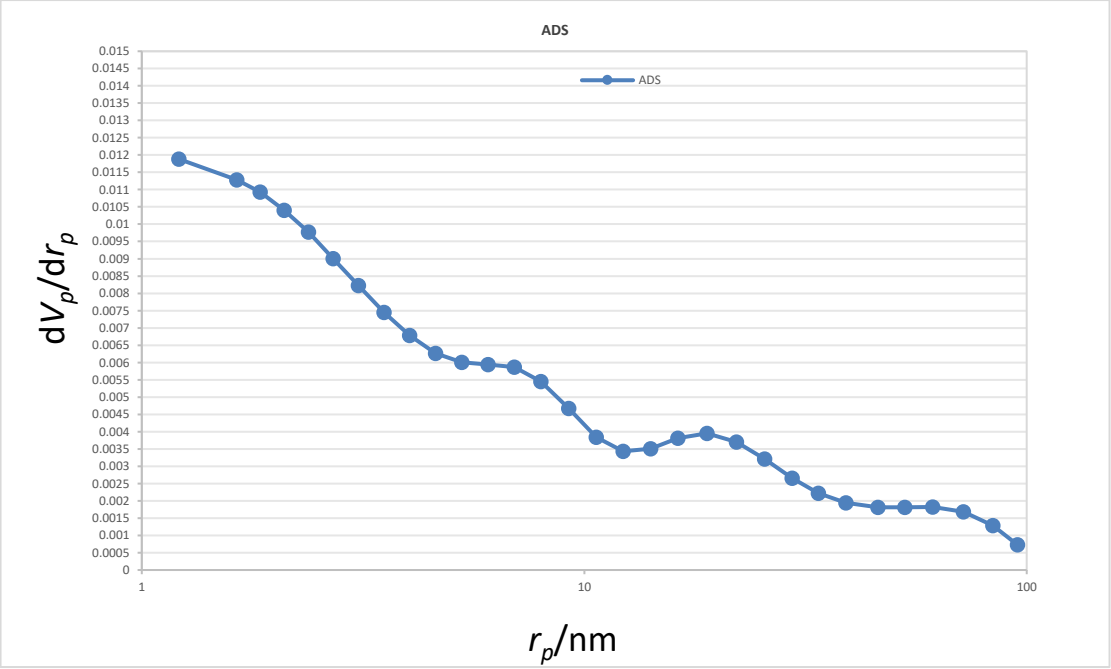



**Figure 11**. Adsorption and desorption isotherm of nitrogen on amorphous silica of high purity

### 3.5. Yield Rate of Synthetic Silica

From 25 g of raw colored glass waste, the highest extraction rate of high-purity silica (99%) was achieved with a product weight of 17.77 g, while the lowest yield rate resulted in the highest loss percentage (2.01%), as shown in **Table 4**. There are three main causes of these losses: mechanical loss, alkali volatilization, and acid solubility **[55-57]**. Our study (98.59%) is better than **[16]** (98.3%) and **[58]** (60.26%).

**Table 4:** Yield rate of synthetic high purity from colored waste glass

| Raw glass waste | Weight of raw glass (g) | Weight of synthetic silica (g) | $SiO_2$ in raw glass % | $SiO_2$ in raw glass % | Yield ratio % | Losses rate % |
|---|---|---|---|---|---|---|
| White | 25 | 17.77 | 71.11 | 99.01 | 99 | 1 |
| Green | 25 | 17.26 | 69.75 | 98.95 | 97.99 | 2.01 |
| Brown | 25 | 17.20 | 68.95 | 98.94 | 98.77 | 1.23 |
| **Average** | **25** | **17.41** | **69.94** | **99** | **98.59** | **1.41** |

The synthesized silica exhibited a specific surface area of 53.04 $m^2/g$, comparable to commercial low-surface-area fumed silica grades like AEROSIL OX 50, which typically range from $50 \pm 15$ $m^2/g$ . With a 99% $SiO_2$ purity, the product aligns with high-purity silica grades

on the market, which generally boast purities exceeding 99%. These characteristics render the produced silica suitable for numerous industrial uses, including as fillers in polymers and elastomers, additives in coatings and paints, and in construction materials. Furthermore, its nanoscale particle size, approximately 9 nm, and mesoporous structure make it ideal for catalytic support and adsorption applications **[59]**.

## 4. Conclusions

As a result of the study, colored glass waste (white, green, and brown) has been successfully recycled, and high-purity silica has been synthesized at 500 C° by alkaline fusion with sodium hydroxide (NaOH), with an average yield rate of 98.59% and a loss rate of 1.41%. X-ray diffraction analysis verified that the product was pure and lacked any secondary crystalline phases, confirming the product is amorphous and free of residual impurities. Nevertheless, low-intensity reflections are observed between 31 and 33°, which may be due to baseline effects or residual trace crystallizations and do not affect the overall amorphous nature of the samples. The final product contained 99% silica, compared to 69.94% in raw glass waste. The accompanying impurities ($Fe_2O_3$, $Al_2O_3$, MgO, and $SO_3$) significantly decreased to less than 1%, demonstrating that this technique is effective regardless of the color of the waste. In contrast, it appears that iron oxides remain difficult to remove even though trace amounts of iron are present. BET analysis showed that the synthetic silica produced had a surface area of 53.04 $m^2/g$, indicating its nanoscale nature and potential adsorption efficiency. The final product has a mesoporous structure, as evidenced by the mean pore diameter (22.585 nm) and the total pore volume (0.263 $cm^3/g$), making it suitable for selective filtration and catalysis. It is confirmed that the monolayer volume (68.5 $cm^3/g$) corresponds to the calculated surface area. An analysis by BJH confirmed the mesoporous nature of the structure, with pore volume 0.261 $cm^3/g$ and mesopore surface area 52.93 $m^2/g$. With its mesoporous structure and specific surface area (53.04 m2/g), synthesized silica shows potential for a variety of applications, including polymer fillers, catalyst supports, and heavy-metal adsorption. The current study, however, did not evaluate its performance in these applications .

There are some limitations to the study, notably the lack of an evaluation of the product's performance in the proposed practical applications. Moreover, iron oxide residues persist in the final product, which calls for improved purification steps. The effectiveness of washing and the removal of sodium chloride residues was not evaluated by electrical conductivity

measurements. The performance of synthesized silica in practical applications (for example, heavy metal adsorption and catalysis) should be evaluated in the future; the process for removing iron oxide needs to be optimized; and industrial-scale production needs to be considered. Electrical conductivity measurements are also recommended in future studies to confirm washing efficacy. The surface morphology and particle size of the prepared silica should also be evaluated using scanning electron microscopy (SEM), and the nature of chemical bonds should be determined through Fourier transform infrared spectroscopy (FTIR). To confirm the accuracy of the product's purity, the next studies should also include ICP-OES or ICP-MS analysis as a complementary measure. A future study should include statistical replications and formal statistical analysis, which are not included in this study.

The results indicate that recycling colored glass waste can yield high-quality silica with surface properties comparable to AEROSIL® 50.**Data Availability**

The data used to support the findings of this study are available from the corresponding author upon request.

**Conflicts of Interest**

No conflicts of interest to declare

**Funding Statement**

No funding is associated with this study.

**5. References**

**[1]** V. Chaitanya and F. Zenhausern. Introduction: Perspective on Water. *Technology & Innovation*. 2015, 17(1–2): pp. 1–3. https://doi.org/10.3727/194982415X14349917064711

**[2]** J. H. Butler and P. D. Hooper. Glass Waste. *Waste: A Handbook for Management*. 2019, pp. 307–322. https://doi.org/10.1016/B978-0-12-815060-3.00015-3

**[3]** D. Wilson et al. Global waste management outlook. 2022.

**[4]** K. S. Gerace and J. C. Mauro. Characterization of soda–lime silicate glass bottles to support recycling efforts. *International Journal of Ceramic Engineering & Science*. 2024, 6(3): pp. 1–11. https://doi.org/10.1002/ces2.10217

**[5]** Y.-C. Baek, C. Real, H. D. Kim, and Y.-C. Jang. Exploring glass recycling: Trends, technologies, and future trajectories. *Environmental Engineering Research*. 2025, 30(3). https://doi.org/10.4491/eer.2024.241

**[6]** A. Soto Trujillo, D. Ddiba, M. Neama, and N. Dhahir. Assessing the conditions for circularity and entrepreneurship for urban sanitation and waste management in Basrah City. *Stockholm Environment Institute*.

**[7]** A. A. K. Abbas, W. S. Al-Rekabi, and Y. T. Yousif. Integrated Solid Waste Management for Urban Area in Basrah District. *Journal of Babylon University/Pure and Applied Sciences*. 2016, 24(3): pp. 666–675.

**[8]** M. B. O. Beneth C. Chukwudi. Glass Recycling: Achieving a Compromise between Economics of Production and Environmental Benefit. *International Journal of Research and Review*. 2019, 6(6): pp. 391–396.

**[9]** G. Gaustad, C. Wilkinson, D. Saadatpour, A. Potter, R. Pao, L. G. Gabrielle, W. Collin, S. Deniz, P. Arron, P. River, M. Scott, and L. Greiner. Glass sustainability: challenges and opportunities at end of life. *Physics and Chemistry of Glasses: European Journal of Glass Science and Technology Part B*. 2025, 66(4): p. 113. https://doi.org/10.13036/17533562.66.4.AM01

**[10]** R. Siikamäki, "Glass can be recycled forever: CRT glass as a raw material for ceramics and glass design," Ph.D. dissertation, School of Arts, Design and Architecture, Aalto Univ., Helsinki, Finland, Sep. 2006.

**[11]** S. P. Varma and D. N. Singh. Influence of curing regimes on strength development of slag-waste glass-based binary geopolymer. *Environmental Science and Pollution Research*. 2025, 32: pp. 634–656. https://doi.org/10.1007/s11356-024-35794-2

**[12]** D. H. A. Besisa, H. H. Mohamed, E. M. M. Ewais, Y. M. Z. Ahmed, and A. M. M. Amin. Synthesis of new $Cr_2O_3$/$Fe_2O_3$/glass composites from industrial wastes; from undesired to advanced optical products. *Environmental Science and Pollution Research*. 2022, 29(56): pp. 84357–84365. https://doi.org/10.1007/s11356-022-21694-w

**[13]** M. B. Ishaq, A. S. Mohammed, and A. A. Mohammed. Novel exploration of chemical compounds in mono-variate, Bi-variate, and multi-variate scenarios of waste glass powder as a cement replacement in concrete. *Sustainable Chemistry and Pharmacy*. 2025, 43: p. 101894. https://doi.org/10.1016/j.scp.2024.101894

**[14]** I. Fanderlik, *Silica Glass and Its Application*, ser. Glass Science and Technology, vol. 11. Amsterdam, The Netherlands: Elsevier, 2013. [Online]. Available: https://shop.elsevier.com/books/silica-glass-and-its-application/fanderlik/978-0-444-98755-6

**[15]** J. E. Shelby, Introduction to Glass Science and Technology, 2nd ed. Cambridge, U.K.: *Royal Society of Chemistry*, 2005. https://doi.org/10.1039/9781847551160

**[16]** H. Mori. Extraction of silicon dioxide from waste colored glasses by alkali fusion using sodium hydroxide. *Journal of the Ceramic Society of Japan*. 2003, 111(1294): pp. 376–381. https://doi.org/10.2109/jcersj.111.376

**[17]** M. Asadikiya and A. C. Powell. Low-Cost Clean One-Step Production of Solar Silicon from Natural Quartzite. *ECS Meeting Abstracts*. 2023, MA2023-01(21): p. 1535. https://doi.org/10.1149/MA2023-01211535mtgabs

**[18]** R. E. Nugraha et al. Recent strategy on green synthesis of mesoporous silica from waste for a sustainable and circular economy. *Journal of Environmental Chemical Engineering*. 2025, 13(5): p. 118288. https://doi.org/10.1016/j.jece.2025.118288

**[19]** R. Zushi, Y. Hayashi, T. Yamanaka, and H. Takizawa. Facile room temperature synthesis of size-controlled spherical silica from silicon metal via simple sonochemical process. *Ultrasonics Sonochemistry*. 2024, 107: p. 106913. https://doi.org/10.1016/j.ultsonch.2024.106913

**[20]** X. Zhang, M. Lu, M. A. M. Idrus, C. Crombie, and V. Jegatheesan. Performance of precipitation and electrocoagulation as pretreatment of silica removal in brackish water and seawater. *Process Safety and Environmental Protection*. 2019, 126: pp. 18–24. https://doi.org/10.1016/j.psep.2019.03.024

**[21]** Munasir, Triwikantoro, M. Zainuri, and Darminto. Synthesis of $SiO_2$ nanopowders containing quartz and cristobalite phases from silica sands. *Materials Science-Poland*. 2015, 33(1): pp. 47–55. https://doi.org/10.1515/msp-2015-0008

**[22]** Munasir, Triwikantoro, M. Zainuri, and Darminto. Ekstraksi dan sintesis nanosilika berbasis pasir bancar dengan metode basah. *Jurnal Penelitian Fisika dan Aplikasinya (JPFA)*. 2013, 3(2): pp. 1–12. https://doi.org/10.26740/jpfa.v3n2.p12-17

**[23]** K. N. Maamur, U. S. Jais, and S. Y. S. Yahya. Magnetic Phase Development of Iron Oxide–$SiO_2$ Aerogel and Xerogel Prepared using Rice Husk Ash as Precursor. *AIP Conference Proceedings*. 2010, 1217(1): pp. 294–301. https://doi.org/10.1063/1.3377832

**[24]** J. Y. Park, Y. M. Gu, J. Chun, B. I. Sang, and J. H. Lee. Pilot-scale continuous biogenic silica extraction from rice husk by one-pot alkali hydrothermal treatment and ball milling. *Chemical and Biological Technologies in Agriculture*. 2023, 10(1): pp. 1–7. https://doi.org/10.1186/s40538-023-00479-4

**[25]** S. N. Ishmah, M. D. Permana, M. L. Firdaus, and D. R. Eddy. Extraction of Silica from Bengkulu Beach Sand using Alkali Fusion Method. *PENDIPA Journal of Science Education*. 2020, 4(2): pp. 1–5. https://doi.org/10.33369/pendipa.4.2.1-5

**[26]** S. Chandrasekhar, K. G. Satyanarayana, P. N. Pramada, P. Raghavan, and T. N. Gupta. Processing, properties and applications of reactive silica from rice husk - An overview. *Journal of Materials Science*. 2003, 38(15): pp. 3159–3168. https://doi.org/10.1023/A:1025157114800

**[27]** J. Xia et al. Synergistic alkali fusion-acid leaching strategy for silica aerogel synthesis from fly ash and performance optimization. *Scientific Reports*. 2025, 15(1): pp. 1–11. https://doi.org/10.1038/s41598-025-24059-8

**[28]** G. Elineema et al. Quantitative recovery of high purity nanoporous silica from waste products of the phosphate fertilizer industry. *Journal of Industrial and Engineering Chemistry*. 2013, 19(1): pp. 63–67. https://doi.org/10.1016/j.jiec.2012.07.003

**[29]** E. Chammas, D. Panias, M. Taxiarchou, G. N. Anastassakis, and I. Paspaliaris. Removal of iron and other major impurities from silica sand for the production of high added value materials. *Proc. IX Balkan Mineral Processing Congress*. 2001, pp. 289–295.

**[30]** F. M. Saleem, H. T. Khreebsh, and S. M. Altaher. Assessment of heavy metals pollution in polluted soils in Basrah city, Iraq. *Basrah Journal of Science*. 2026, 44(1): pp. 356–371. https://doi.org/10.29072/basjs.20260119

**[31]** M. G. Iskander, J. Lai, C. J. Oswald, and R. J. Mannheimer. Development of a Transparent Material to Model the Geotechnical Properties of Soils. *Geotechnical Testing Journal*. 1994, 17(4): pp. 425–433. https://doi.org/10.1520/GTJ10303J

**[32]** F. W. M. Al-Halfi. Mineralogy, geochemistry and industrial assessment of sand dunes, Missan Governorate, southeast of Iraq. *M.S. thesis, Department of Earth Sciences, College of Science, University of Basrah, Basrah, Iraq*. 2022.

**[33]** S. J. Al-Khafaji, F. W. Al-Halfi, and H. K. Jasim. Assessment of sand dunes in Missan Governorate, South-eastern Iraq: Implications for Extraction High Purity Silica. *IOP Conference Series: Earth and Environmental Science*. 2024, 1300(1): p. 012016. https://doi.org/10.1088/1755-1315/1300/1/012016

**[34]** L. Silvia and M. Zainuri. Analisis Silika ($SiO_2$) Hasil Kopresipitasi Berbasis Bahan Alam menggunakan Uji XRF dan XRD. *Jurnal Fisika dan Aplikasinya*. 2020, 16(1): p. 12. https://doi.org/10.12962/j24604682.v16i1.5322

**[35]** S. Hadi, Munasir, and Triwikantoro. Sintesis Silika Berbasis Pasir Alam Bancar menggunakan Metode Kopresipitasi. *Jurnal Fisika dan Aplikasinya*. 2011, 7(2): p. 110202.

**[36]** S. A. Ajeel, K. A. Sukkar, and N. K. Zedin. Extraction of high purity amorphous silica from rice husk by chemical process. *IOP Conference Series: Materials Science and Engineering*. 2020, 881(1): p. 012096. https://doi.org/10.1088/1757-899X/881/1/012096

**[37]** R. Sharafudeen, J. M. Al-Hashim, M. O. Al-Harbi, A. I. Al-Ajwad, and A. A. Al-Waheed. Preparation and Characterization of Precipitated Silica using Sodium Silicate Prepared from Saudi Arabian Desert Sand. *Silicon*. 2017, 9(6): pp. 917–922. https://doi.org/10.1007/s12633-016-9531-8

**[38]** J. Rouquerol, D. Avnir, D. H. Everett, C. Fairbridge, M. Haynes, N. Pernicone, and K. Unger. Guidelines for the characterization of porous solids. *Studies in Surface Science and Catalysis*. 1994, 87: pp. 1–9. https://doi.org/10.1016/S0167-2991(08)63059-1

**[39]** N. A. P. Caraos. Parametric analysis of silica extraction process via alkaline fusion and hydrothermal desilication methods from municipal solid waste bottom ash derived from direct combustion. *Unpublished thesis, University of the Philippines Los Baños*. 2018.

**[40]** U. Kalapathy, A. Proctor, and J. Shultz. A simple method for production of pure silica from rice hull ash. *Bioresource Technology*. 2000, 73(3): pp. 257–262. https://doi.org/10.1016/S0960-8524(99)00127-3

**[41]** K. Atamnia, S. Satha, H. Satha, and M. F. Gonon. Synthesis, structural and thermal characterization of silica glasses containing BaO, SrO and ZnO oxides. *Materials Research Express*. 2021, 8(1): p. 015201. https://doi.org/10.1088/2053-1591/abd33c

**[42]** F. M. Fudzi, H. M. Kamari, F. D. Muhammad, A. A. Latif, and Z. Ismail. Structural and Optical Properties of Zinc Borotellurite Glass Co-Doped with Lanthanum and Silver Oxide. *Journal of Materials Science and Chemical Engineering*. 2018, 6(4): pp. 18–23. https://doi.org/10.4236/msce.2018.64003

**[43]** A. Kaur, A. Khanna, and F. González. DSC and Raman studies of silver borotellurite glasses. *AIP Conference Proceedings*. 2016, 1731(1): p. 070002. https://doi.org/10.1063/1.4947868

**[44]** B. E. Warren. X-ray Diffraction Study of the Structure of Glass. *Chemical Reviews*. 1940, 26(2): pp. 237–255. https://doi.org/10.1021/cr60084a007

**[45]** A. S. Al-Maliki, D. A. Al-Abbawy, and Z. A. Abdulnabi. High-efficiency adsorption and sustainable desorption of anionic dyes using a novel AC–$Fe_2O_3$/ZnO nanocomposite. *Basrah Journal of Science*. 2026, 44(1): pp. 393–419. https://doi.org/10.29072/basjs.20260121

**[46]** G. Gorni. X-ray absorption spectroscopy for the study of glasses and glass-ceramics for optical applications: A comprehensive review. *Ceramics International*. 2025, 51(30, Part A): pp. 62157–62187. https://doi.org/10.1016/j.ceramint.2025.11.122

**[47]** A. Paul. Chemistry of Glasses. *Chapman and Hall, London & New York*, 2nd ed. 1982.

**[48]** J. E. Shelby. Introduction to Glass Science and Technology. *Royal Society of Chemistry*. 2020.

**[49]** A. K. Varshneya. Fundamentals of Inorganic Glasses. *Elsevier*. 2013.

**[50]** R. K. Iler. The Chemistry of Silica: Solubility, Polymerization, Colloid and Surface Properties, and Biochemistry. *John Wiley & Sons, New York, NY*. 1979.

**[51]** C. J. Brinker and G. W. Scherer. Sol–Gel Science: The Physics and Chemistry of Sol–Gel Processing. *Academic Press*. 1990.

**[52]** W. Trabelsi, M. Benzina, and S. Bouaziz. Physico-chemical characterisation of the Douiret sand (Southern Tunisia): Valorisation for the production of Silica Gel. *Physics Procedia*. 2009, 2(3): pp. 1461–1467. https://doi.org/10.1016/j.phpro.2009.11.117

**[53]** J. L. Gurav, I. K. Jung, H. H. Park, E. S. Kang, and D. Y. Nadargi. Silica aerogel: Synthesis and applications. *Journal of Nanomaterials*. 2010, 2010: p. 409310. https://doi.org/10.1155/2010/409310

**[54]** M. Thommes, K. Kaneko, A. V. Neimark, J. P. Olivier, F. Rodriguez-Reinoso, J. Rouquerol, and K. S. Sing. Physisorption of gases, with special reference to the evaluation

of surface area and pore size distribution (IUPAC Technical Report). *Pure and Applied Chemistry*. 2015, 87(9–10): pp. 1051–1069. https://doi.org/10.1515/pac-2014-1117

**[55]** R. G. C. Beerkens and O. S. Verheijen. Reactions of alkali vapours with silica based refractory in glass furnaces, thermodynamics and mass transfer. *Glass Technology*. 2005, 46(6): pp. 371–382.

**[56]** D. C. Hurd and K. Takahashi. On the estimation of minimum mechanical loss during an in situ biogenic silica dissolution experiment. *Marine Micropaleontology*. 1983, 7(5): pp. 441–447. https://doi.org/10.1016/0377-8398(83)90010-3

**[57]** J. Madejová and P. Komadel. Comparative FT-IR study of structural modifications during acid treatment of dioctahedral smectites and hectorite. *Spectrochimica Acta Part A: Molecular Spectroscopy*. 1998, 54(10): pp. 1397–1406. https://doi.org/10.1016/S1386-1425(98)00040-7

**[58]** P. Ussawanawachat, N. Nawaukkaratharnant, and A. Theerapapvisetpong. Synthesis and characterization of silica nanoparticles from solar panel glass cullet. *Journal of Metals, Materials and Minerals*. 2025, 35(4): p. e2448. https://doi.org/10.55713/jmmm.v35i4.2448

**[59]** N. Hewitt. Compounding Precipitated Silica in Elastomers: Theory and Practice. *William Andrew Publishing, Norwich, NY, USA*. 2007.

## تحضير السيليكا غير المتبلورة عالية النقاء من نفايات الزجاج الملون بطريقة الانصهارر القلوي

**فادية وليد الحلفي[1] وحارث عبد الحليم السعد[1]**

### المستخلص

تُعدّ السيليكا عالية النقاء مادة ذات قيمة كبيرة للصناعات الحديثة نظرًا لخصائصها الفريدة. في المقابل، تُشكّل نفايات الزجاج الملون مصدرًا للتلوث البيئي ويصعب إعادة تدويرها. لذا، يُمثّل الحصول على السيليكا من مصادر مستدامة تحديًا صناعيًا وبيئيًا. باستخدام طريقة الصهر القلوي (وهي طريقة اقتصادية ومنخفضة الطاقة نسبيا)، تهدف هذه الدراسة لتحويل نفايات الزجاج الملون إلى سيليكا عالية النقاء. تضمنت هذه الطريقة غمر نفايات الزجاج المسحوق في حمض الهيدروكلوريك بتركيز 2 مولاري لمدة 24 ساعة. ثم تحضير سيليكات الصوديوم الصلبة بتسخين 20 غرامًا من نفايات الزجاج المنقى مع 80 غرامًا من هيدروكسيد الصوديوم عند 500 درجة مئوية لمدة ساعتين. يُخلط محلول سيليكات الصوديوم مع حمض الهيدروكلوريك بتركيز 3 مولاري لتكوين حمض السيليسيك. تستغرق عملية المعالجة 18 ساعة، تليها عملية ترشيح وتجفيف لمدة 48 ساعة. أكدت تقنية حيود الأشعة السينية (XRD) الطبيعة غير المتبلورة للمنتج. وكشف التحليل الكيميائي أن المنتج النهائي يحتوي على 99% من السيليكا، مقارنةً بـ 69.94% في نفايات الزجاج الخام، بمعدل إنتاجية 98.59%. ولوحظ انخفاض ملحوظ في الشوائب. ($Fe_2O_3$, $Al_2O_3$, MgO, and $SO_3$) وأظهر تحليل BET مساحة سطحية نوعية (53.04 م²/غ) وحجم مسام إجمالي منخفض (0.263 سم³/غ). وأكد تحليل BJH الطبيعة المسامية المتوسطة، حيث بلغ حجم المسام 0.261 سم³/غ ومساحة سطح المسام المتوسطة 52.93 م²/غ. وكانت هذه العملية مستقرة مع جميع ألوان نفايات الزجاج، مما يشير إلى إمكانية استخدامها في التطبيقات الصناعية وتطبيقات المواد النانوية المسامية.

**الكلمات المفتاحية:** نفايات الزجاج الملون، اعادة التدوير، الانصهار القلوي، سليكا عالية النقاوة، مساحة سطحية.